Electronic Supplementary Information (ESI) for:

Electronic defect states at the $LaAlO_3/SrTiO_3$ heterointerface revealed by O K-edge X - ray absorption spectroscopy

Natalia Palina[a,b,†], Anil Annadi[b,e], Teguh Citra Asmara[a,b,c], Caozheng Diao[a], Xiaojiang Yu[a], Mark B. H Breese[a,c], T. Venkatesan[b,c,d], Ariando[b,c,†], Andrivo Rusydi[a,b,c,†]

a. Singapore Synchrotron Light Source, National University of Singapore, Singapore 117603, Singapore.

b. NUSNNI-Nanocore, National University of Singapore, Singapore 117411, Singapore.

c. Department of Physics, National University of Singapore, Singapore 117542, Singapore.

d. Department of Electrical and Computer Engineering, National University of Singapore, Singapore 117576, Singapore

e. Department of Physics and Astronomy, University of Pittsburgh, Pittsburgh, Pennsylvania, 15260, USA

† natalie.mueller@nus.edu.sg, phyarian@nus.edu.sg, phyandri@nus.edu.sg.

Supporting Figures

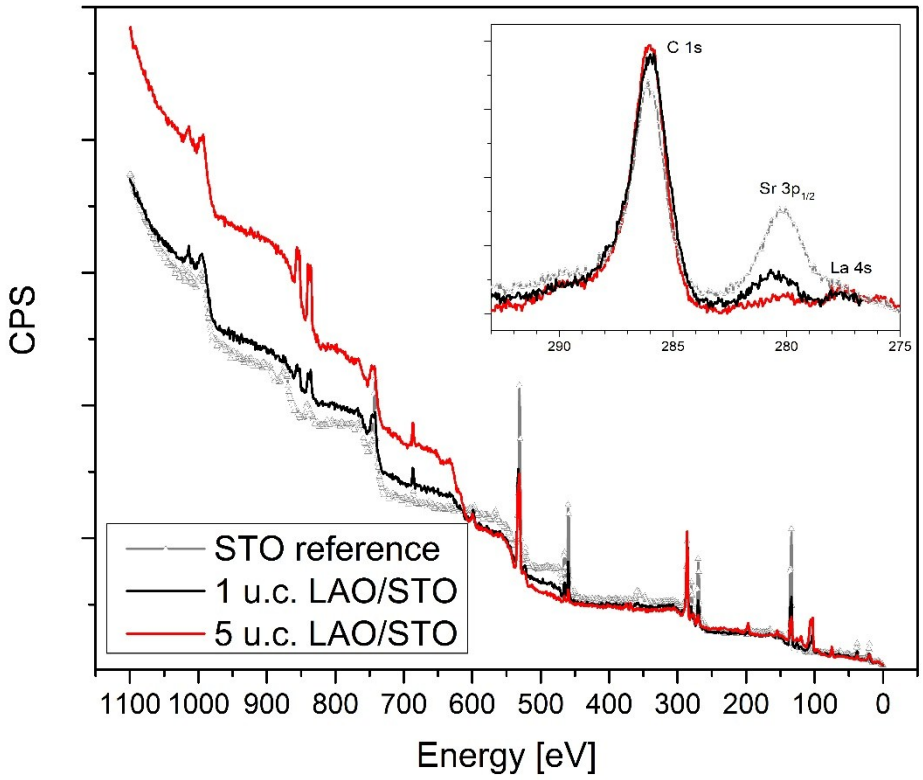

Figure ESI 1: XPS survey scan from insulating (black), conducting (red) and reference STO samples (triangle scatters). Inset shows details of experimental C 1*s* photoelectron region. Note that observed carbon signal are very similar for both investigated LAO/STO samples and pSTO reference. Hence, we assuming that the origin of carbon peak in XPS related to the C-tape used to mount samples onto sample holder.

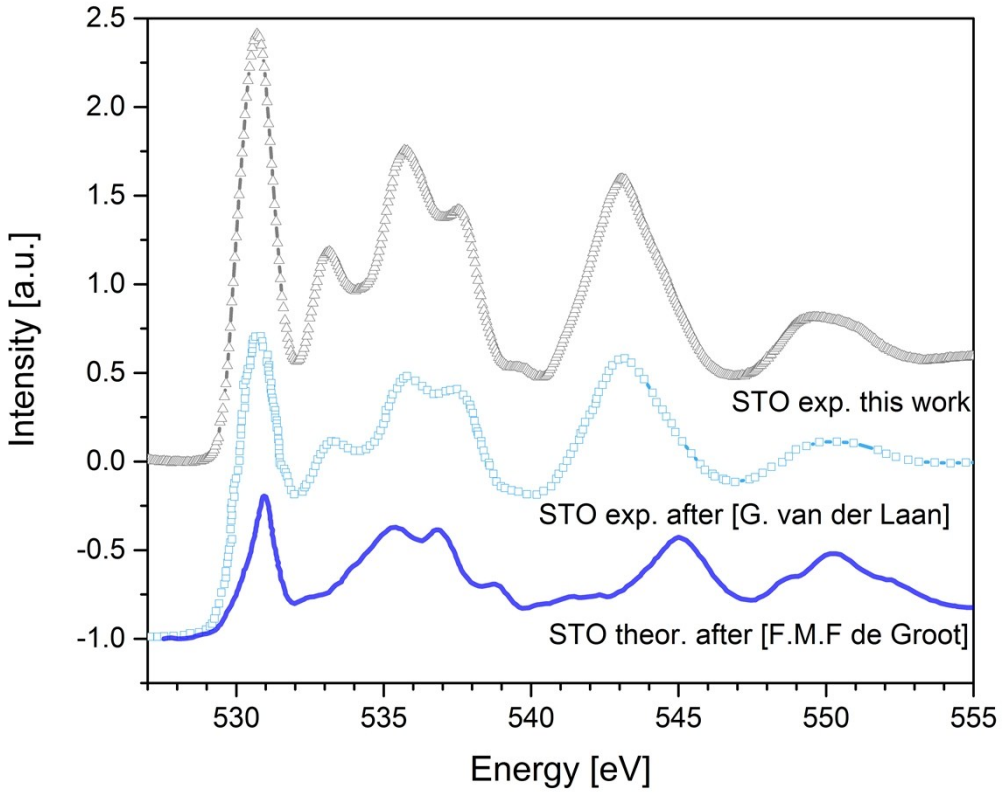

Figure ESI 2: Comparison of the O *K*–edge XANES spectra for STO reference used in this work (grey triangle scatters) with experimental STO spectrum published by [G. van der Laan] (light blue square scatters) and *p*-projected density of states (blue solid line) adopted from [F. M. F. de Groot]. It is obvious that, experimental STO spectrum used in this work, which carbon contaminated no (i) misleading structure, (ii) broadening of spectral features or (iii) noticeable change in the energy position of main peaks which can be assigned to carbon-oxide contamination. Therefore, we conclude that in our analysis changes observed in O *K*–edge XANES are originated from the thickness dependent changes at the LAO/STO hetero*interface.* Note that thickness dependent changes for 1 u.c and 5 u.c LAO/STO samples in current work (see Figure 1, manuscript) are similar to the data previously reported elsewhere [J.-S. Lee].

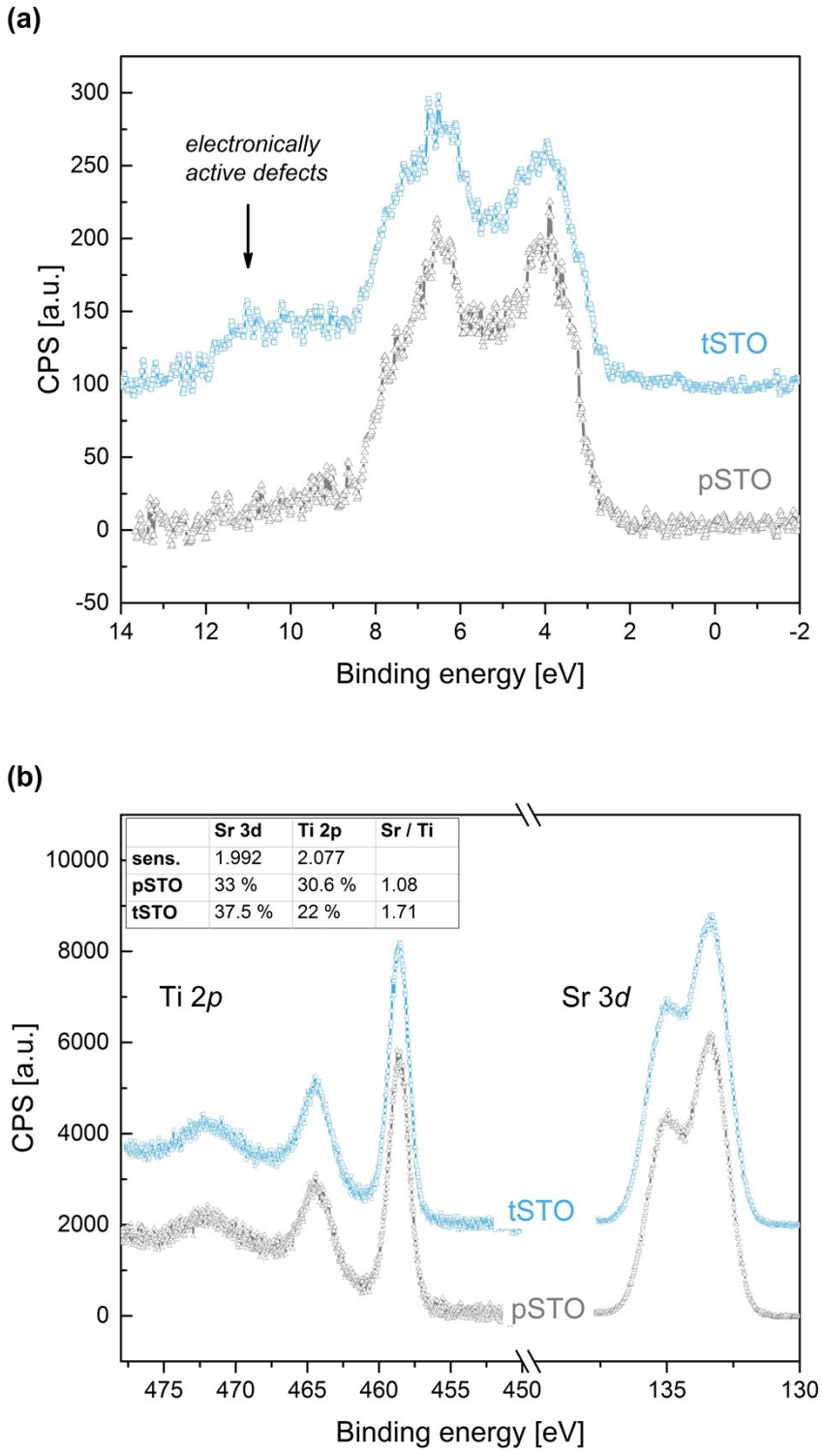

Figure ESI 3: (a) Normal emission resonant valence band XPS spectra for the pristine STO (pSTO triangle scatters) and TiO_2 terminated STO (tSTO, square scatters). The electronically active defects appeared at the bottom of the valence band, around 11 eV. Energy position is consistent with position of peak 1 observed in XANES data and with data reported elsewhere. [S. A. Chambers]. (b) XPS signal of Ti 2p and Sr 3d for pSTO and tSTO respectively. The inserted table show relative concentration of Ti and Sr as well as respective ratio of these elements. Enhancement of Sr / Ti ratio in case of tSTO can be attributed to the presence of Sr adatoms or SrO islands at the tSTO surface.

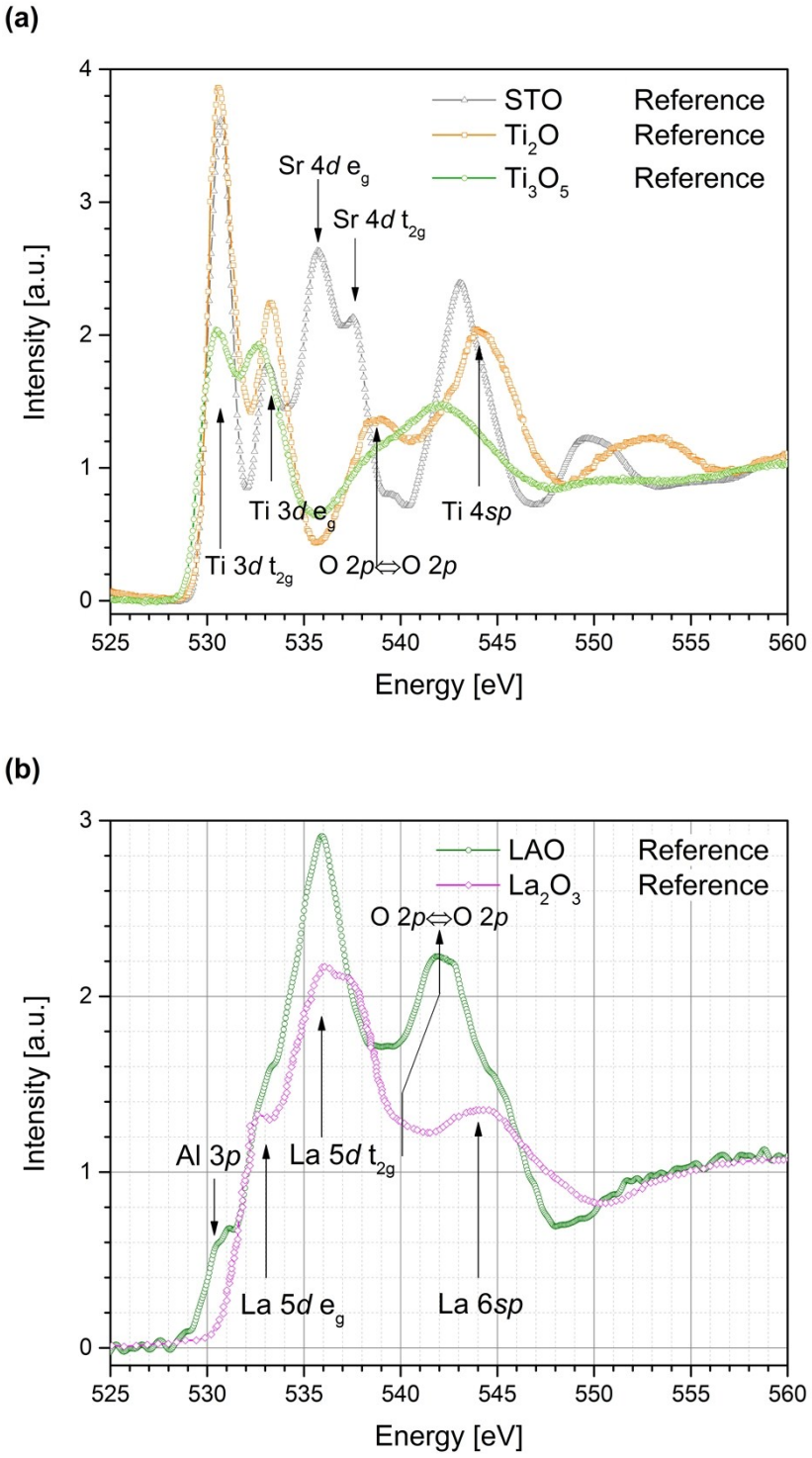

Figure ESI 4: O *K*–edge XANES spectra of **(a)** reference TiO_2 (orange, anatase phase), STO (grey) and Ti_3O_5 (light green) compounds and **(b)** La_2O_3 (magenta, adopted from [J.G. Chen]) and LAO (green) compounds. Spectra are acquired with experimental settings identical to 1 and 5 u.c. LAO/STO samples. O *K*–edge XANES spectra of TiO_2 and La_2O_3 are used for fingerprint analysis in order to identify energy position of main transitions. See Table 1 for details.

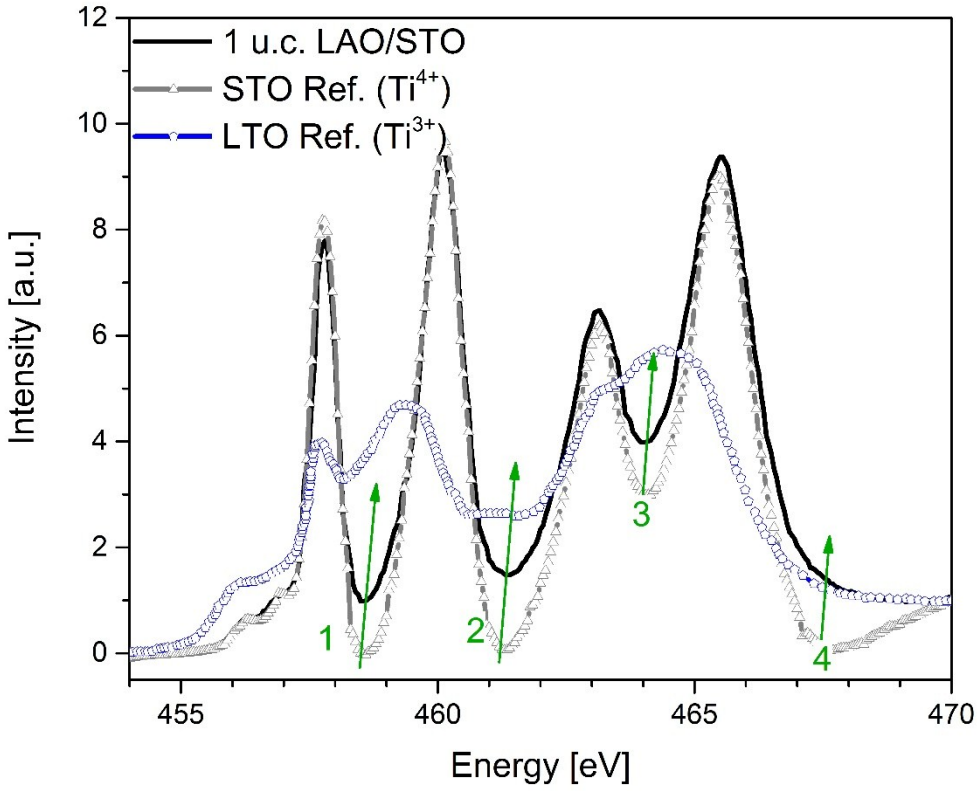

Figure ESI 5: Ti L_{32}-edge XANES spectrum of insulating 1 u.c. (black) sample along with pSTO reference (triangle scatters, this work) and LTO reference (circle scatters, adapted from [M. Abbate] XANES spectra. Increased intensity of valley 1-4 in insulating LAO/STO sample indicates presence of the *noninteger valence state* of Ti. Arrows are guideline for eye, marking maxima of the peaks observed in the reference LTO (Ti^{3+}) reference spectra.

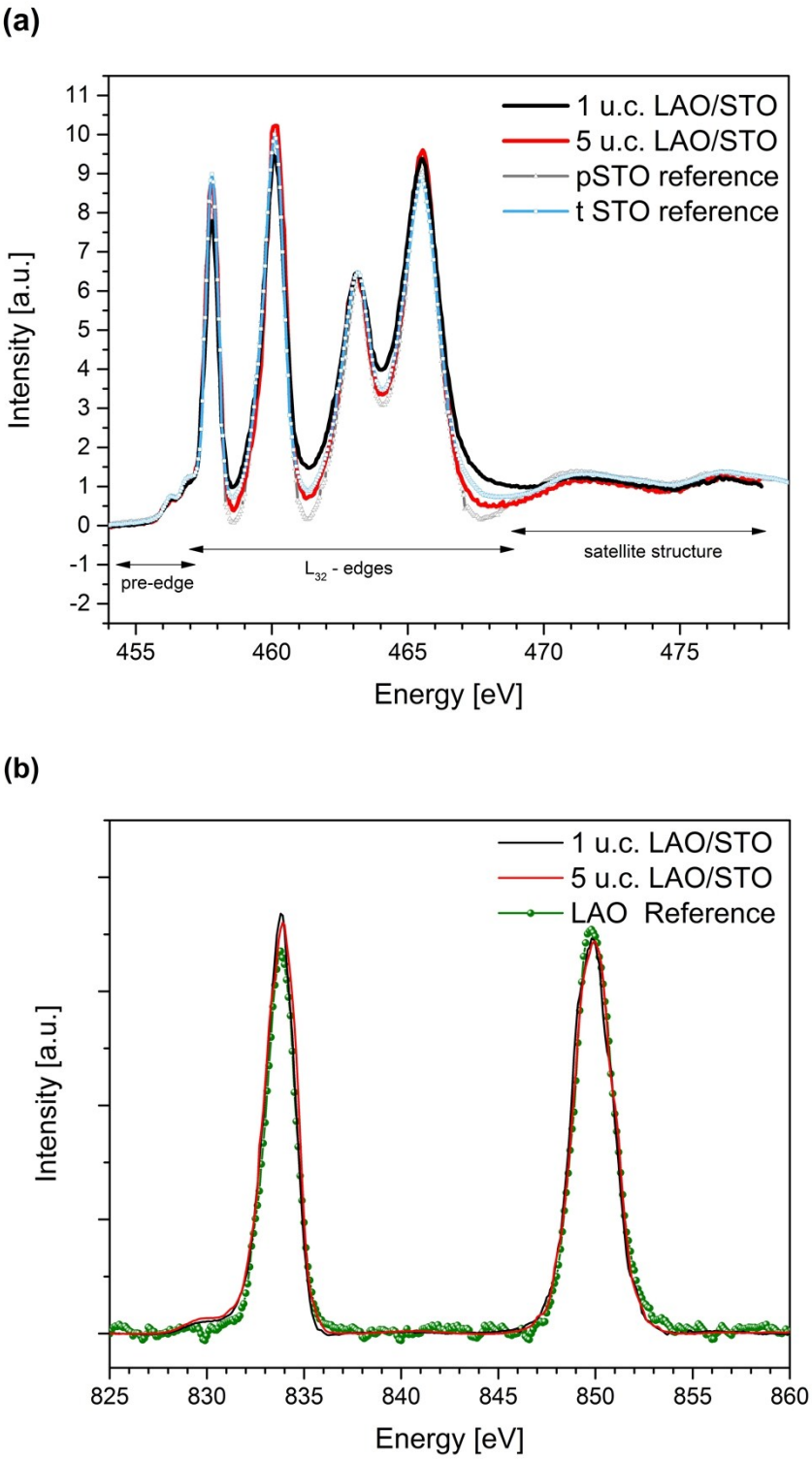

Figure ESI 6: (a) Ti L_{32}-edge XANES spectra of insulating 1 u.c. (black) and conducting 5 u.c. (red) samples along with STO references XANES spectrum (triangle scatters). (b) La $M_{5,4}$-edge XANES spectra of insulating 1 u.c. (black) and conducting 5 u.c. (red) samples along with LAO reference (circle scatters). La atoms seemed to experience least changes as a function of LAO thickness.

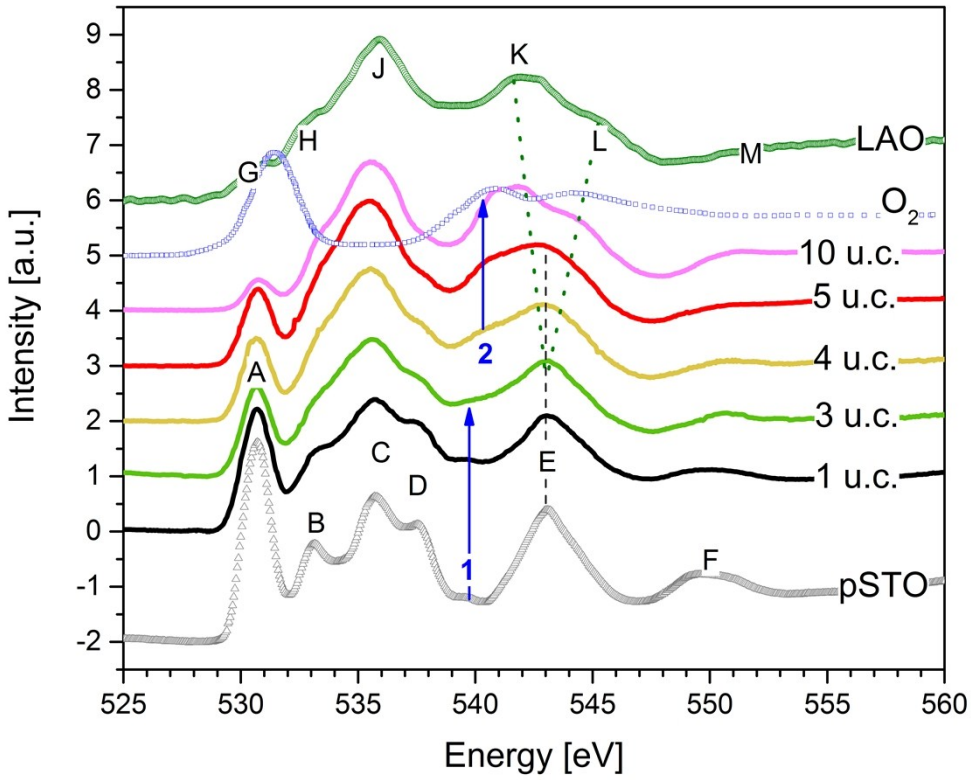

Figure ESI 7: Thickness dependence of O *K*-edge XANES spectra and pristine STO and LAO reference spectra. XANES signal clearly differs from STO reference at LAO thickness above 4 u.c. Dashed line at 543 eV mark energy position of O 2p – Ti 4sp transition (peak E). Dotted lines indicate broadening of peak E due to larger weight of LAO (peaks K and L) contribution to XANES signal. Unique, defect-induced states, are marked as peak 1 and peak 2, in accordance to the manuscript notations. For LAO thicknesses below critical defect-induced states (peak 1) identified as localized charge at Ti ions with noninteger valence state. For LAO thicknesses above critical, defect-induced states (peak 2) as delocalized charge with pronounced O 2p- O 2p character, refer to the XANES spectrum of molecular oxygen (blue scatters). The energy position of peak 2 match well with the position of the σ* peak observed in the molecular-like oxygen spectrum. For LAO thickness above critical, Overall broadening of main shape-resonances reflects presence of oxygen defects, e.g. delocalized electrons. Observed broadening of O K-edge XANES shape-resonances is due to reduced lifetime in the resonant process and disorder in the local coordination caused by defects.

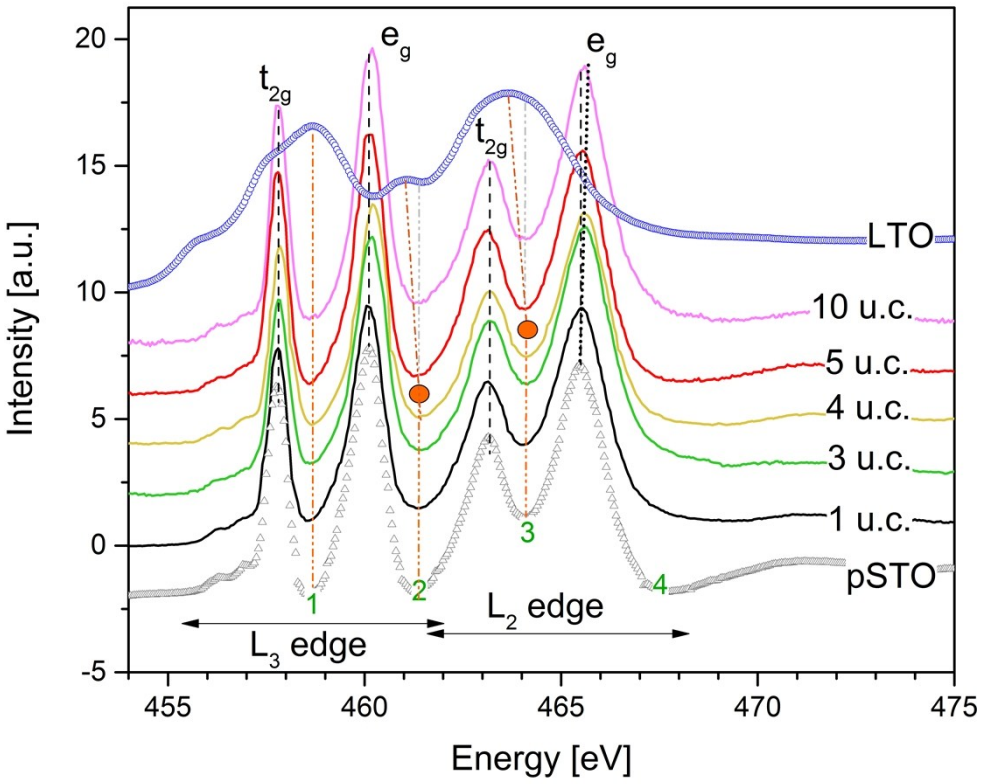

Figure ESI 8: Thickness dependence of Ti L_{32}-edge XANES spectra, pSTO reference (triangle scatters, this work) and LTO reference (circle scatters, adapted from [11]). With no noticeable shift of Ti t2g and eg transitions (see dashed lines, at both edges) an increased intensity of valley 1-4 indicates presence of the *noninteger valence state* of Ti. Above critical thickness (marked by filled circle), energy position of valley 1-4 is gradually shifting towards the maxima of the main peaks observed in the reference LTO (Ti^{3+}) reference spectra. This indicates presence of Ti^{3+} states, in accordance to previously reported data. Additionally, we observe increased t_{2g} and e_g orbital splitting, most pronounced at L_2 edge. These facts pointing to electronic reconstruction and presence of complex ground state ($3d^0$ and $3d^1$) for conducting LAO samples.

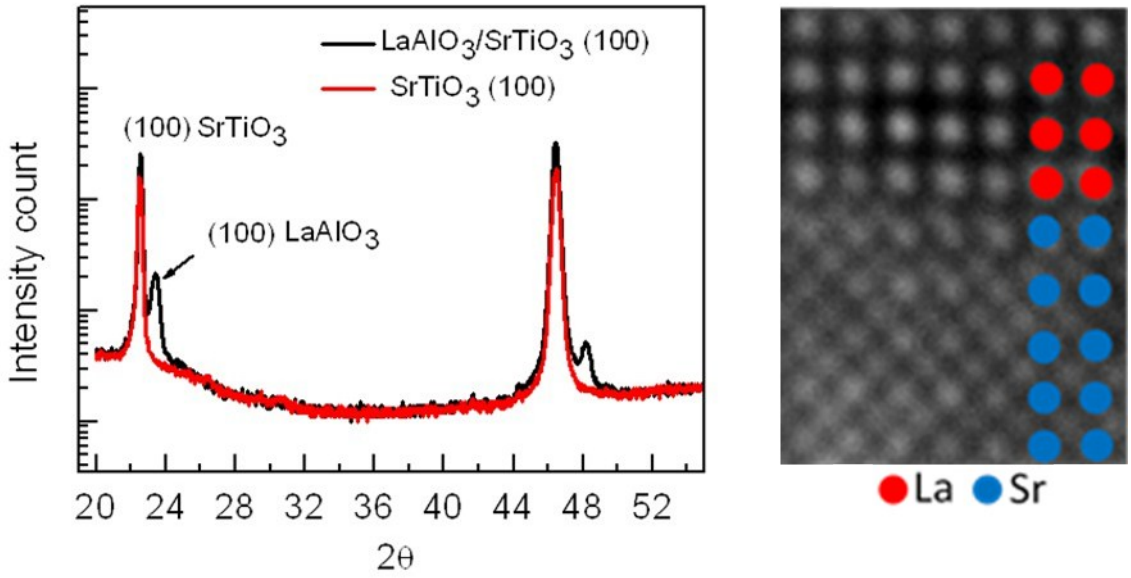

Figure ESI 9: (left) XRD graph of LAO (15nm)/STO thin film, confirms the single phase and epitaxial growth of LAO on STO. (right) Cross-section TEM for (001) LAO/STO interfaces, where La are denoted by red circle at LAO side and Sr is denoted by blue circle at STO side. These thin films were deposited at relatively high oxygen partial pressures of $1x10^{-3}$ Torr, and at laser energy density of 1.2 J/cm^2 with substrate to target distance of 6 cm in PLD, which combinedly produce a plasma that allows us to prepare films with minimal reacting effects such as surface sputtering and chemical reactivity on the substrate surfaces.

Table 1: Main resonance transitions observed in oxygen *K*-edge XANES spectra for reference compounds and unique defect-induced transitions characteristic for insulating (peak 1) and conducting (peak 2) LAO/STO samples. For the reference compounds used here, assignment of resonance transitions is in a good agreement with available calculations and previously reported experimental data. Note: symbol "⇔" means hybridization

Peak	**Main Resonance transitions**	**Photon energy [eV]**
$SrTiO_3$ reference (sc)		
A	O 1s → O 2p ⇔ Ti 3d t2g	530.70
B	O 1s → O 2p ⇔ Ti 3d eg	533.15
C	O 1s → O 2p ⇔ Sr 4d eg	535.70
D	O 1s → O 2p ⇔ Sr 4d t2g	537.55
E	O 1s → O 2p ⇔Ti 4sp	543.05
F	O 1s → O 2p ⇔Ti 4sp / O 2p ⇔ O 2p	549.70
$LaAlO_3$ reference (sc)		
G	O 1s → O 2p ⇔ Al 3p	530.70
H	O 1s → O 2p ⇔La 5d eg	533.00
J	O 1s → O 2p ⇔ La 5d t2g	535.95
K	O 1s → O 2p ⇔ O 2p	541.95
L	O 1s → O 2p ⇔ La 6sp	545.00
M	O 1s → O 2p ⇔La 6sp/ O 2p ⇔ O 2p	552.00
Peak	**Unique defect-induced transitions**	**Photon energy [eV]**
1 u.c. $LaAlO_3$ / $SrTiO_3$ (insulating sample)		
1	O 1s → O 2p ⇔ O 2p	539.60
5 u.c. $LaAlO_3$ / $SrTiO_3$ (conducting sample)		
2	O 1s → O 2p (σ*)	540.50

Supporting References

[de Groot F. M. F.] *Phys. Rev. B* **48**, 2074 (1993)

[G. van der Laan] *Phys. Rev. B*, **41**, 12366 (1990)

[J.-S. Lee] *Nat. Mater*., **12**, 703-706 (2013)

[S. A. Chambers] *Surface Science*, **606**, 554–558 (2012)

[J.G. Chen] *Surface Science Reports* **30**, 1-152 (1997)

[M. Abbate] *Phys. Rev. B* **44**, 5419-5422 (1991)